RESEARCH ARTICLE

WILEY

Plasmodium berghei sporozoites in nonreplicative vacuole are eliminated by a PI3P-mediated autophagy-independent pathway

Annina Bindschedler[1,2] | Rahel Wacker[1,2] | Jessica Egli[1] | Nina Eickel[1,2] | Jacqueline Schmuckli-Maurer[1] | Blandine M. Franke-Fayard[3] | Chris J. Janse[3] | Volker T. Heussler[1]

[1]Institute of Cell Biology, University of Bern, Bern, Switzerland

[2]Graduate School for Cellular and Biomedical Sciences, University of Bern, Bern, Switzerland

[3]Leiden malaria group, Department of Parasitology, Leiden University Medical Center, Leiden, The Netherlands

Correspondence
Volker T. Heussler, Institute of Cell Biology, University of Bern, Bern, Switzerland.
Email: heussler@izb.unibe.ch

Funding information
Schweizerischer Nationalfonds zur Förderung der Wissenschaftlichen Forschung, Grant/Award Number: 310030_182465

Abstract

The protozoan parasite *Plasmodium*, causative agent of malaria, invades hepatocytes by invaginating the host cell plasma membrane and forming a parasitophorous vacuole membrane (PVM). Surrounded by this PVM, the parasite undergoes extensive replication. Parasites inside a PVM provoke the *Plasmodium*-associated autophagy-related (PAAR) response. This is characterised by a long-lasting association of the autophagy marker protein LC3 with the PVM, which is not preceded by phosphatidylinositol 3-phosphate (PI3P)-labelling. Prior to productive invasion, sporozoites transmigrate several cells and here we describe that a proportion of traversing sporozoites become trapped in a transient traversal vacuole, provoking a host cell response that clearly differs from the PAAR response. These trapped sporozoites provoke PI3P-labelling of the surrounding vacuolar membrane immediately after cell entry, followed by transient LC3-labelling and elimination of the parasite by lysosomal acidification. Our data suggest that this PI3P response is not only restricted to sporozoites trapped during transmigration but also affects invaded parasites residing in a compromised vacuole. Thus, host cells can employ a pathway distinct from the previously described PAAR response to efficiently recognise and eliminate *Plasmodium* parasites.

KEYWORDS
autophagy, elimination, liver stage, Plasmodium, transient vacuole

1 | INTRODUCTION

Malaria is a devastating disease caused by the protozoan parasite *Plasmodium*. Before the symptomatic blood infection, the parasite undergoes clinically silent replication in hepatocytes. *Plasmodium* sporozoites are injected into the human body by an infectious *Anopheles* mosquito and migrate to the liver via the blood circulation. They enter the liver tissue by crossing the endothelium (Tavares et al., 2013). Before invading their final host cells and undergoing liver stage development, sporozoites traverse several hepatocytes (Mota et al., 2001).

Annina Bindschedler and Rahel Wacker contributed equally to this work.

During cell traversal, sporozoites enter hepatocytes either through cell wounding or through invagination of the host cell plasma membrane, thereby forming a transient vacuole (TV). Sporozoites then exit these nonreplicative TVs to avoid degradation by host cell lysosomes (Mota et al., 2001; Risco-Castillo et al., 2015). The micronemal protein Sporozoite microneme Protein Essential for Cell Traversal 2 (SPECT2, also called PLP1) is essential for sporozoite cell traversal, as its pore-forming activity is responsible for entering cells through cell wounding and for exiting TVs (Amino et al., 2008; Ishino, Chinzei, & Yuda, 2005; Ishino, Yano, Chinzei, & Yuda, 2004; Risco-Castillo et al., 2015). After traversing several cells, sporozoites establish infection through productive invasion of a liver cell. This involves invagination of the host cell plasma membrane, leading to the formation of a parasitophorous vacuole (PV). Productive invasion of a liver cell depends on secretion of proteins from the secretory organelles, rhoptries and micronemes, of the sporozoite. These proteins allow the formation of a moving junction complex (Besteiro, Dubremez, & Lebrun, 2011; Risco-Castillo et al., 2015). The moving junction is thought to act as a molecular sieve to exclude host cell proteins from the forming parasitophorous vacuole membrane (PVM; Amino et al., 2008; Spielmann, Montagna, Hecht, & Matuschewski, 2012). The PVM is considerably remodelled by the parasite and is the main interface between the host cell cytoplasm and the parasite. Export of proteins to the PVM and maintenance of PVM integrity are crucial for successful development of the parasite in the hepatocyte. Inside the PV, the sporozoite rounds up, transforms into the growing liver stage trophozoite and then undergoes repeated nuclear division events, resulting in a large multinuclear schizont. By continuous invagination of the schizont membrane, daughter merozoites are formed. They are then released into the host cell cytoplasm upon rupture of the PVM, followed by ordered cell death of the host cell. Merozoite release induces the formation of merosomes, merozoite-filled vesicles, that bud off from the dying host cell into an adjacent blood vessel. Once merosomes burst, free merozoites invade red blood cells, thus initiating the symptomatic blood stage infection (Sturm et al., 2006).

Only around half of the invaded sporozoites successfully complete the development into liver schizonts: the other half is eliminated by the host cell (Prado et al., 2015). It is not well understood which factors contribute to either survival or elimination of an individual parasite. Recently, it has been shown by us and others that host cell autophagy-related processes influence the development of liver stages (Boonhok et al., 2016; Prado et al., 2015; Real et al., 2018; Thieleke-Matos et al., 2016; Wacker et al., 2017; Zhao et al., 2016). Autophagy-related processes acting as intracellular immune responses against liver stages have recently been summarised under the term *Plasmodium*-associated autophagy-related (PAAR) responses (Agop-Nersesian, Niklaus, Wacker, & Heussler, 2018). Autophagy is a catabolic process of the cell that ensures cell survival under stress conditions. Cytosolic substrates are engulfed in double-membraned vesicles called autophagosomes and subsequently degraded upon autophagosome–lysosome fusion. In canonical autophagy, starvation triggers a signalling cascade, activating the Unc51-like autophagy activating kinase (ULK) complex that initiates autophagosome formation

(Mizushima, 2010). The ULK complex further activates a class III phosphatidylinositol 3-kinase (PI3KC3) which converts phosphatidylinositol (PI) to phosphatidylinositol 3-phosphate (PI3P) in the ER membrane (Russell et al., 2013; Volinia et al., 1995). There it is thought to recruit downstream factors and provide a platform for autophagosome formation through induction of a pre-autophagosomal structure, the omegasome (Axe et al., 2008; Walker, Chandra, Manifava, Axe, & Ktistakis, 2008). The elongation of the forming autophagosomal membrane from the omegasome requires complex membrane dynamics depending on the ATG12 and LC3 ubiquitin-like conjugation systems. Concerted actions of these systems mediate the conjugation of cytosolic LC3 (LC3-I) to phosphatidylethanolamine (PE), forming lipidated and membrane-associated LC3-II (reviewed in [Nakatogawa, 2013]). In addition to the canonical autophagy pathway, there are autophagy-related processes that only involve certain steps or proteins of the canonical pathway. An autophagy-related process that is able to control intracellular pathogens is LC3-associated phagocytosis (LAP). LAP can be used to target vacuole-borne intracellular pathogens such as *Salmonella typhimurium* (Huang et al., 2009; Sanjuan et al., 2007). Importantly, LAP differs from canonical autophagosome formation in its initiation: it is independent of the ULK complex and does not involve *de novo* membrane formation but still involves the formation of PI3P in the phagosomal membrane by the PI3KC3 complex. As in canonical autophagy, events downstream of PI3P generation include the recruitment of the ubiquitin-like conjugation systems, incorporation of LC3 into the phagosomal membrane and degradation of phagosomal contents through fusion with lysosomes.

In hepatocytes infected with the rodent malaria parasite *Plasmodium berghei*, the majority of parasites exhibit a prolonged labelling of the PVM with LC3 (Grutzke et al., 2014; Prado et al., 2015; Thieleke-Matos et al., 2016; Wacker et al., 2017). Recently, we have shown that this LC3-labelling follows a noncanonical autophagy pathway, independent of the ULK complex, but dependent on the ubiquitin-like conjugation systems (Wacker et al., 2017). While some parasites are eliminated by this autophagy-related pathway, many parasites can escape the host cell autophagic targeting and are able to complete development into liver schizonts.

Here we investigated whether LC3-labelling of the PVM of the *P. berghei* liver stage during PAAR response follows a LAP-like pathway that involves PI3P formation at the PVM. Interestingly, in the majority of *P. berghei*-infected host cells, long-lasting LC3-association with the PVM occurred independently of PI3P and is thus distinct from LAP. However, some parasites became strongly positive for PI3P directly after entering the host cell. Our analyses revealed that these are mainly traversing sporozoites in nonreplicative TVs. We followed PI3P-positive sporozoites by time-lapse imaging and show that they are efficiently eliminated through lysosomal acidification in an autophagy-independent manner. Thus, we can now distinguish two host cell responses against early liver stage parasites: on the one hand, long-lasting LC3-association with the PVM during the PAAR response, and on the other hand PI3P-associated elimination of sporozoites in traversing vacuoles or parasites surrounded by a compromised PVM.

2 | RESULTS

2.1 | Long-lasting LC3 association with the PVM is independent of PI3P

During canonical autophagy and LAP, PI3P-labelling precedes the action of the two ubiquitination systems that recruit and lipidate LC3 at the target membrane. To investigate the role of PI3P in LC3-association with the PVM during the PAAR response, we made use of a specific reporter of PI3P, the FYVE motif. In this system, two adjacent FYVE motifs fused to a fluorescent protein allow visualisation of PI3P in membranes (Gillooly et al., 2000). To allow combinations with other live stains, we used either GFP-2xFYVE or mCherry-2xFYVE, which were confirmed to show the same localisation (Figure S1). First, we co-expressed mCherry-2xFYVE and GFP-LC3 in HeLa cells and infected them with non-fluorescent wild-type *P. berghei* parasites (*Pb*WT) as both channels (green and red) for optimal live imaging were already occupied. However, since the vast majority of intracellular parasites provoke a PAAR response (Prado et al., 2015; Schmuckli-Maurer et al., 2017; Wacker et al., 2017), we could detect live parasites by positive LC3-labelling of their vacuole membrane. Although this experimental approach did not allow an overall quantification of invaded parasites with a positive PI3P membrane labelling as it excludes the small LC3-negative parasite population, it still allowed analysis of whether the PAAR response is preceded by PI3P-formation at the vacuole membrane. Interestingly, initiating live cell imaging immediately upon addition of sporozoites to the cells and following parasites until they became positive for LC3, we did not observe association of mCherry-2xFYVE preceding the PAAR response (Figure 1a and Movie S1). This suggests that the incorporation of LC3 into the vacuole membrane does not require PI3KC3 activity and might thus follow a pathway distinct from LAP. Supporting this assumption, treatment of infected cells with the PI3KC3 inhibitor wortmannin did not lead to reduced LC3 association with the PVM (Figure 1b,c). To confirm the inhibitory effect of wortmannin, we treated non-infected GFP-2xFYVE-expressing cells with wortmannin and observed a complete loss of membrane-associated GFP-2xFYVE (Figure S2). In summary, our observations in *P. berghei*-infected host cells indicate that the PAAR response can function independently of PI3P-formation at the PVM, and therefore differs substantially from a LAP-like pathway. However, since not all parasites provoke a PAAR response, we asked whether PAAR-negative parasites respond differently in terms of PI3P-labelling and what the nature of these PAAR-negative parasites is.

2.2 | The vacuolar membrane of a proportion of parasites does become PI3P-positive

To address the question of whether any intracellular sporozoites become PI3P-positive, we infected HeLa cells expressing the PI3P reporter mCherry-2xFYVE and LC3-GFP with *Pb*WT parasites and followed them for up to 36 hr. Although the majority of parasites were unlabelled by the PI3P reporter in the PVM, confirming the previous observation (Figure 1), we detected some parasites whose surrounding membrane displayed a transient 2xFYVE signal (Figure 2a and Movie S2). To quantify PI3P-positive parasites, we then used mCherry-expressing parasites (*Pb*mCherry) to infect GFP-2xFYVE-expressing HeLa cells. 2xFYVE-positive parasites were counted at different time points and revealed a peak of PI3P-positive parasites of around 6% at 1.5 hr post infection (hpi), whereas at later time points, the 2xFYVE signal was detectable in 2% or less of all infected cells (Figure 2b). To exclude cell line specific effects, we repeated the experiment in HuH7 cells, a human hepatoma cell line. Importantly, also in HuH7 cells, a similar number of 2xFYVE-positive parasites was detected 1.5 hpi (Figure S3a). Having confirmed that the PI3P response is not cell line dependent, the next experiments were performed in HeLa cells only. Interestingly, the transient 2xFYVE-labelling was followed by a very weak LC3-labelling that was also transient and lasted approximately 1 hr. This is in stark contrast to the PAAR response, where the majority of sporozoites become strongly positive for LC3 soon after invading their host cell and stay LC3-positive until they have reached the late schizont stage around 2 days post infection. These differences indicate that the 2xFYVE-positive parasites are recognised by a mechanism different to that of the PAAR response. In fact, in some double-infected cells, one sporozoite was recognised by the PAAR response, whereas the other was 2xFYVE-positive (Figure 2c and Movie S3). One possibility is that individual parasites may differ in the composition of their surrounding membrane. This is supported by the fact that the 2xFYVE signal appears to be smooth and evenly distributed around the 2xFYVE-positive parasites, unlike the typical tubovesicular structure of the LC3-positive PVM, which can be observed specifically early after infection.

2.3 | The PI3P-positive membrane surrounding parasites is not a typical PVM

To investigate the nature of the 2xFYVE-positive parasite-surrounding membrane, we infected GFP-2xFYVE-expressing HeLa and HuH7 cells with mCherry-expressing *P. berghei* parasites (*Pb*mCherry) and visualised the PVM as early as 1.5 hpi by antibody staining against the PVM protein "Upregulated in Infective Sporozoites 4" (UIS4; Kaiser, Matuschewski, Camargo, Ross, & Kappe, 2004). We found in both cell lines that 2xFYVE-positive parasites did not show any surrounding UIS4 signal (Figure 3a,b and Figure S3b). This observation indicates that parasites with a 2xFYVE-positive, and hence PI3P-labelled, membrane do not export PVM proteins to this membrane and thus cannot establish a typical PVM. Since PI3P-labelling occurs predominantly very soon after infection, we next tested whether PI3P-positive parasites are still in the process of cell traversal. Cell traversal precedes invasion of a hepatocyte and can either occur by cell wounding or by invagination of the host cell membrane and subsequent formation of a TV membrane around the traversing parasite (Risco-Castillo et al., 2015). To determine if parasites

are free in the host cell cytosol or rather contained within a TV or PV, we made use of the fact that the parasite plasma membrane contains considerably lower cholesterol levels than that of mammalian cells. The cholesterol-binding agent filipin allows detection of host cell plasma membrane-derived vacuoles such as the PVM or TV membrane (Bano, Romano, Jayabalasingham, & Coppens, 2007;

Risco-Castillo et al., 2015) and was therefore used to characterise the 2xFYVE-positive membranes. Interestingly, 2xFYVE-positive parasites showed a clear filipin-labelling that colocalises with the 2xFYVE signal, indicating a surrounding host cell-derived membrane. As expected, the PVM of UIS4-positive parasites shows a similar filipin-labelling (Figure 3c,d) as it consists of a parasite modified host cell membrane.
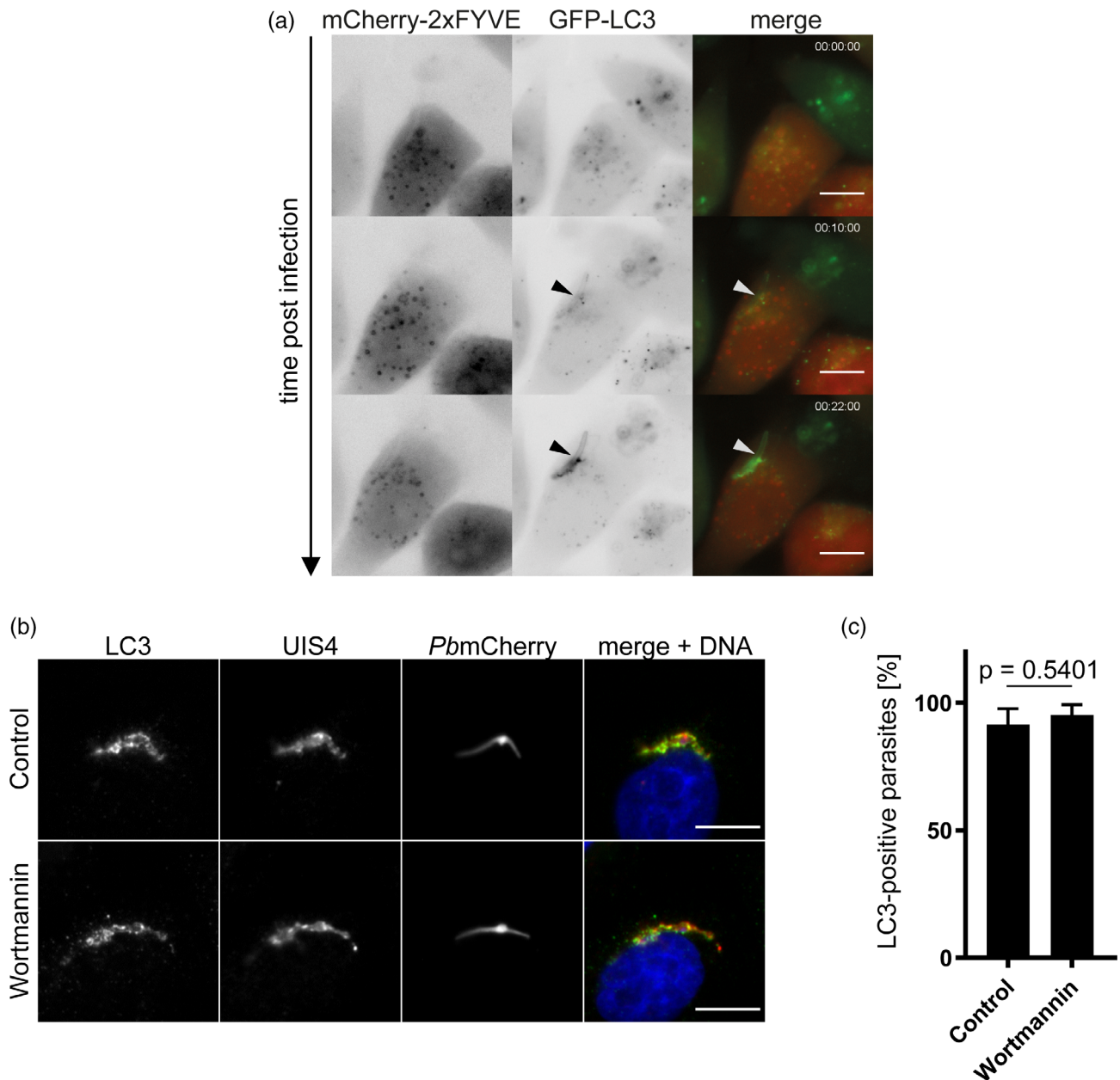

FIGURE 1 LC3-association with the PVM is independent of PI3P. (a) HeLa cells co-expressing mCherry-2xFYVE and GFP-LC3 were infected with *Pb*WT parasites. Immediately after addition of sporozoites, time-lapse microscopy was performed at 30-s intervals. Still images of Movie S1 are depicted. Note that GFP-LC3-labelling of the vacuole membrane is not preceded by the presence of mCherry-2xFYVE. The arrow points towards the wild-type parasite. Time stamps are in hh:mm:ss post infection. $N = 20$. Scale bar: 10 μm (b) HeLa cells were infected with mCherry-expressing *P. berghei* parasites (*Pb*mCherry) in the presence or absence of 2.5 μM Wortmannin. At 4 hpi, cells were fixed and stained with antibodies against host cell LC3 (green) and *P. berghei* UIS4 (red) and DNA was stained with DAPI (blue). The merge does not include the mCherry signal. Scale bar: 10 μm. (c) Quantification of (b). Infected cells each were assessed for the presence of LC3 at the PVM. The graph depicts mean and *SD* of two independent experiments. *p*-Values were calculated using a Student's *t*-test. $N = 100$ in each experiment. Note that wortmannin treatment does not lead to reduced LC3-labelling
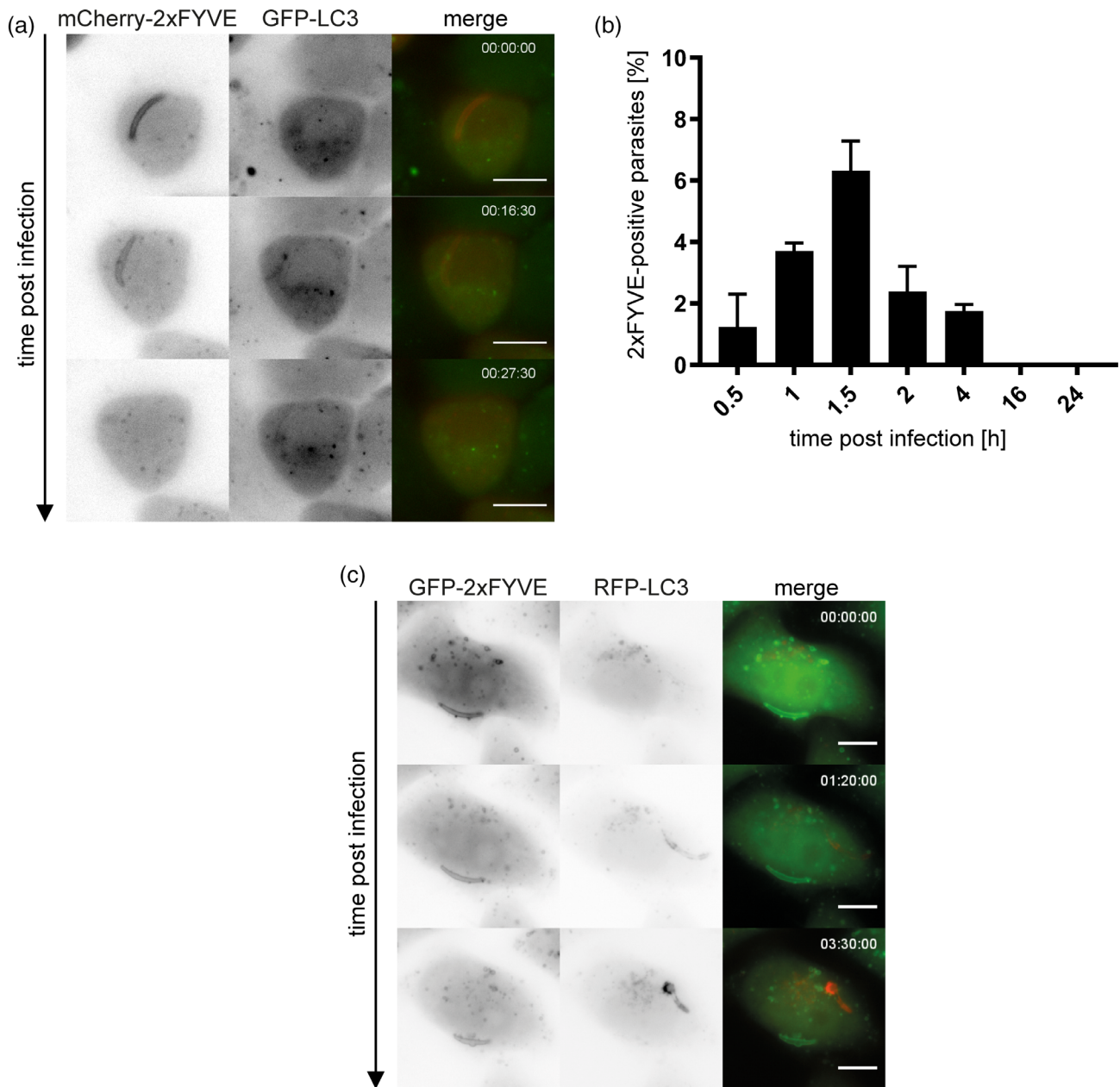
FIGURE 2 A population of parasites become positive for the PI3P indicator 2xFYVE. (a) HeLa cells co-expressing mCherry-2xFYVE and GFP-LC3 were infected with *Pb*WT parasites. Immediately after addition of sporozoites, time-lapse microscopy was performed at 30-s intervals. Still images of Movie S2 are depicted. Note the transient mCherry-2xFYVE-labelling of the parasite that is followed by a very weak, transient GFP-LC3 accumulation. Time stamps are in hh:mm:ss post infection. Scale bar: 10 μm. (b) GFP-2xFYVE-expressing cells were infected with *Pb*mCherry parasites. At the indicated time points, cells were fixed and the percentage of GFP-2xFYVE-positive parasites was determined. The graph depicts the mean and *SD* of three independent experiments. *N* = 50 per timepoint and experiment. (c) GFP-2xFYVE- and RFP-LC3-co-expressing cells were infected with *Pb*WT parasites. Immediately after sporozoite addition, time-lapse microscopy was performed at 10-min intervals. Still images of Movie S3 are depicted. Note that this cell is infected with two parasites, which are differently recognised by the host cell. Time stamps are in hh:mm:ss post infection. Scale bar: 10 μm

However, the membrane of 2xFYVE-positive parasites is smooth, as seen by both 2xFYVE and filipin-labelling, compared to UIS4-positive PVM, which is characterised by tubovesicular structures. To investigate whether the PI3P-positive host cell membrane is a compromised PVM or rather a TV membrane, we next determined whether or not PI3P-labelled parasites have productively invaded their host cell.

Rhoptry Neck Protein 4 (RON4) is a component of the moving junction complex and can be detected at the apical end of non-invaded sporozoites and sporozoites residing in a TV (Risco-Castillo et al., 2014). Thus, we generated a transgenic parasite line that expresses a C-terminal mCherry-tagged version of RON4 (PBANKA_0932000; Figure S4) to distinguish between invaded and
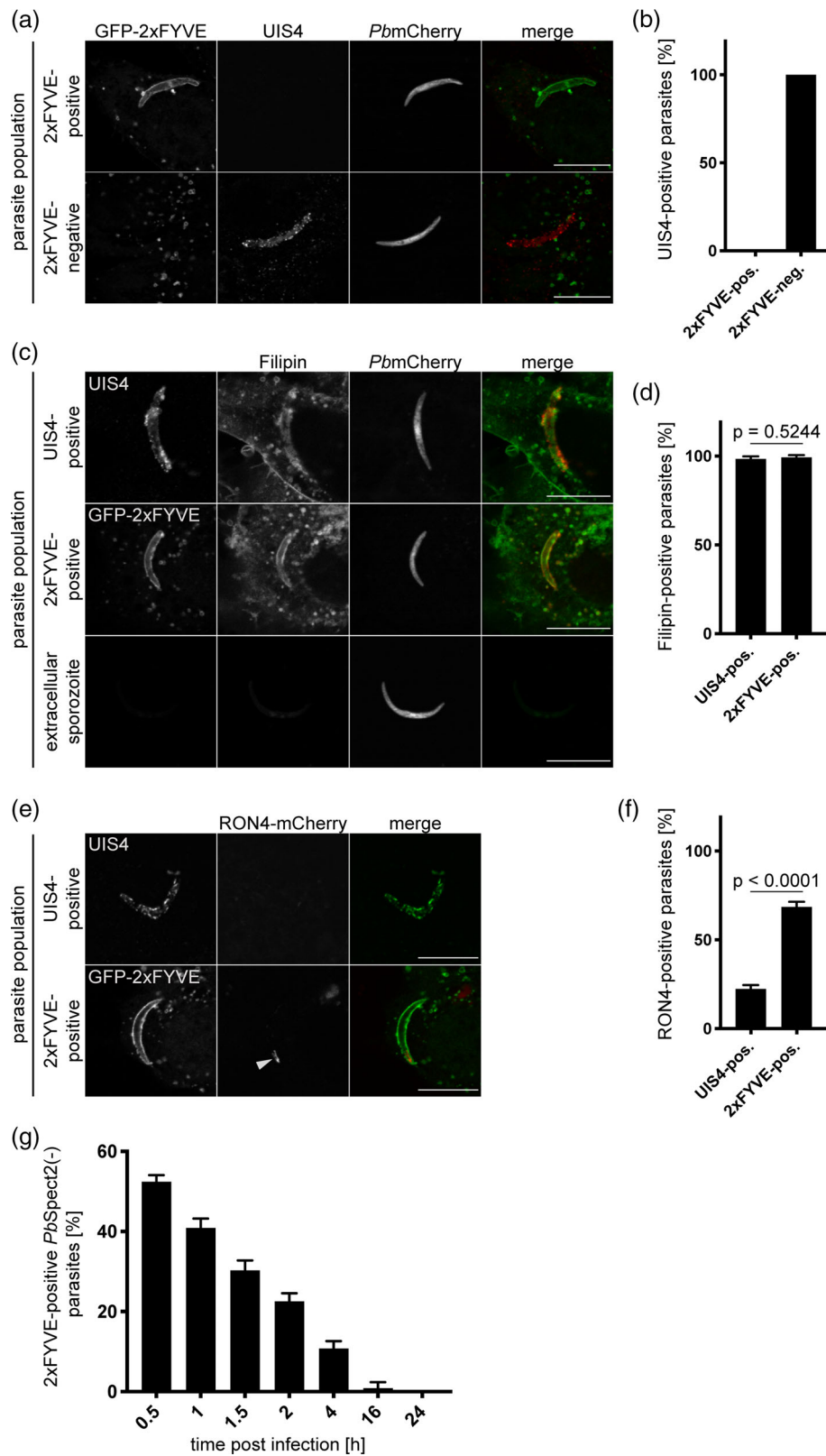
FIGURE 3 Legend on next page.

traversing sporozoites. Parasites residing in a UIS4-positive PVM were considered as successfully invaded. As expected, 1.5 hpi the vast majority of parasites residing in a UIS4-positive PVM showed no apical mCherry signal as a result of discharge of the content of their rhoptries during invasion. In contrast, apical RON4-mCherry could be detected in the majority of the 2xFYVE-positive parasites (Figure 3e,

f). This indicates that many 2xFYVE-positive parasites have not yet discharged their rhoptry content, either because they are contained in a TV during traversal or because they have failed to successfully complete invasion. To further investigate whether the PI3P-positive parasites are sporozoites trapped within TVs, we made use of cell traversal-deficient parasites, *Pb*Spect2(–). These parasites are still able to invade cells *in vitro* either productively or by generation of a TV. If the mutant parasites are contained within a TV they cannot leave the cell because SPECT2 with its membrane attack complex/perforin domain is missing (Kaiser et al., 2004; Risco-Castillo et al., 2015). We hypothesised that there should be an accumulation of PI3P-positive parasites when the sporozoites are not able to exit from their TV. To quantify PI3P-positive *spect2(–)* parasites, we transiently transfected HeLa cells with mCherry-2xFYVE and infected them with GFP-expressing *spect2(–)* sporozoites (*Pb*Spect2(–)F) (Amino et al., 2008; Ishino et al., 2005). 2xFYVE-positive parasites were counted at different timepoints. There was a maximum of around 50% PI3P-positive parasites at 0.5 hpi (Figure 3g), clearly confirming our hypothesis. Compared to cell traversal-competent parasites this is an around 10-fold increase in the percentage of PI3P-positive parasites (Figure 2b). Also, the peak shifted from 1.5 hpi with wild-type parasites to 0.5 hpi for the *spect2(–)* parasites indicating that parasites targeted by PI3P-labelling are indeed sporozoites that fail to exit from their TVs.

2.4 | PI3P-positive parasites are rapidly eliminated

Since PI3P-labelled parasites exhibit signs of failed cell traversal or invasion, we expected them to not successfully develop into liver stage schizonts. Analysis of the fate of mCherry-expressing parasites with a 2xFYVE-positive membrane using time-lapse live imaging indeed showed rapid elimination of these parasites (Figure 4a,b and

Movie S4). To assess whether lysosomes are involved in the elimination of PI3P-positive parasites, we monitored lysosome fusion with the parasite-surrounding membrane by following the localisation of the Lysosome-AssociatedMembrane Protein 1 (LAMP1), an integral lysosome membrane protein. Infection of LAMP1-GFP and mCherry-2xFYVE co-expressing cells infected with *Pb*WT parasites, indeed showed that almost all (more than 95%) parasites with a 2xFYVE-positive membrane became strongly positive for LAMP1 over time (Figure 4c,d and Movie S5). This was followed by shrinkage of the parasite, which most likely indicates parasite death. Although we found a very strong correlation of PI3P and LAMP1 labelling, the experimental setup using unstained *Pb*WT parasites, did not allow to conclude that PI3P labelling is indeed required to attract lysosomes to the membrane.

2.5 | PI3P-positive parasites are acidified independently LAP and autophagy

We next asked whether parasites residing in TVs are targeted by LAP because LAP is also characterised by transient PI3P and LC3-labelling of membranes followed by acidification of the vacuolar content. Since we have already shown that parasites surrounded by a transient PI3P-positive membrane also become weakly and transiently positive for LC3 (Figure 2a), we next determined whether the parasite cytosol becomes acidified. We made use of the fact that GFP, in contrast to mCherry, is sensitive to acidification (Chudakov, Matz, Lukyanov, & Lukyanov, 2010; Patterson, Knobel, Sharif, Kain, & Piston, 1997). Analysing 2xFYVE-positive, GFP-expressing parasites (*Pb*GFP) over time, we found that all parasites lost their fluorescence signal within a few hours (Figure 5a,d and Movie S6). This indeed indicates efficient acidification of the 2xFYVE-positive parasite population. To again exclude that this is a HeLa cell line specific phenomenon, 2xFYVE-positive

---

FIGURE 3 The PI3P-associated host cell response targets parasites in nonreplicative transient vacuoles. (a) GFP-2xFYVE-expressing HeLa cells were infected with *Pb*mCherry parasites. At 1.5 hpi, cells were fixed and stained with an anti-UIS4 antibody (here shown in red). Note that the GFP-2xFYVE-positive parasite does not exhibit a UIS4-positive PVM. The merge does not include the *Pb*mCherry signal. Scale bar: 10 μm. (b) Quantification of (a). Parasites showing a UIS4-positive PVM were counted in the GFP-2xFYVE-positive and -negative populations. The experiment was conducted three times. N = 50 in each experiment. (c) WT or GFP-2xFYVE-expressing (here shown in red) HeLa cells were infected with *Pb*mCherry parasites. At 1.5 hpi, cells were fixed and stained with filipin (here shown in green). Infected WT cells were additionally stained with an anti-UIS4 antibody (shown in red). Extracellular *Pb*mCherry sporozoites were fixed and stained with filipin, which predominantly stains cholesterol-rich host cell membranes. Note that the intracellular parasites, in contrast to extracellular parasites, are surrounded by a filipin-positive membrane of host cell origin. For clarity, the merge does not include the *Pb*mCherry signal of the parasite. Scale bar: 10 μm. (d) Quantification of (c). Parasites surrounded by a filipin-positive vacuole membrane were counted in the GFP-2xFYVE-positive and UIS4-positive parasite populations. The graph depicts mean and *SD* of three independent experiments. *p*-Values were calculated using a Student's *t*-test. N = 50 per experiment. (e) WT or GFP-2xFYVE-expressing HeLa cells were infected with *P. berghei* parasites expressing RON4-mCherry. At 1.5 hpi, cells were fixed and WT cells were stained with an anti-UIS4 antibody (shown in green). The arrow points towards the rhoptries. Note that GFP-2xFYVE-positive parasites have not discharged their rhoptries. Scale bar: 10 μm. (f) Quantification of (e). The percentage of parasites with an apically localised RON4 signal was determined in the GFP-2xFYVE-positive and UIS4-positive parasite populations. The graph depicts mean and *SD* of three independent experiments. *p*-Values were calculated using a Student's *t*-test. N = 50 in each experiment. (g) mCherry-2xFYVE-expressing HeLa cells were infected with *Pb*Spect2(-)F parasites. At the indicated time points, cells were fixed and the percentage of mCherry-2xFYVE-positive parasites was determined. The graph depicts the mean and *SD* of three independent experiments. N = 50 per timepoint and experiment. Note that there are much more (around 50%) 2xFYVE-positive parasites compared to Figure 2b with transmigration competent parasites (around 6% at the maximum)
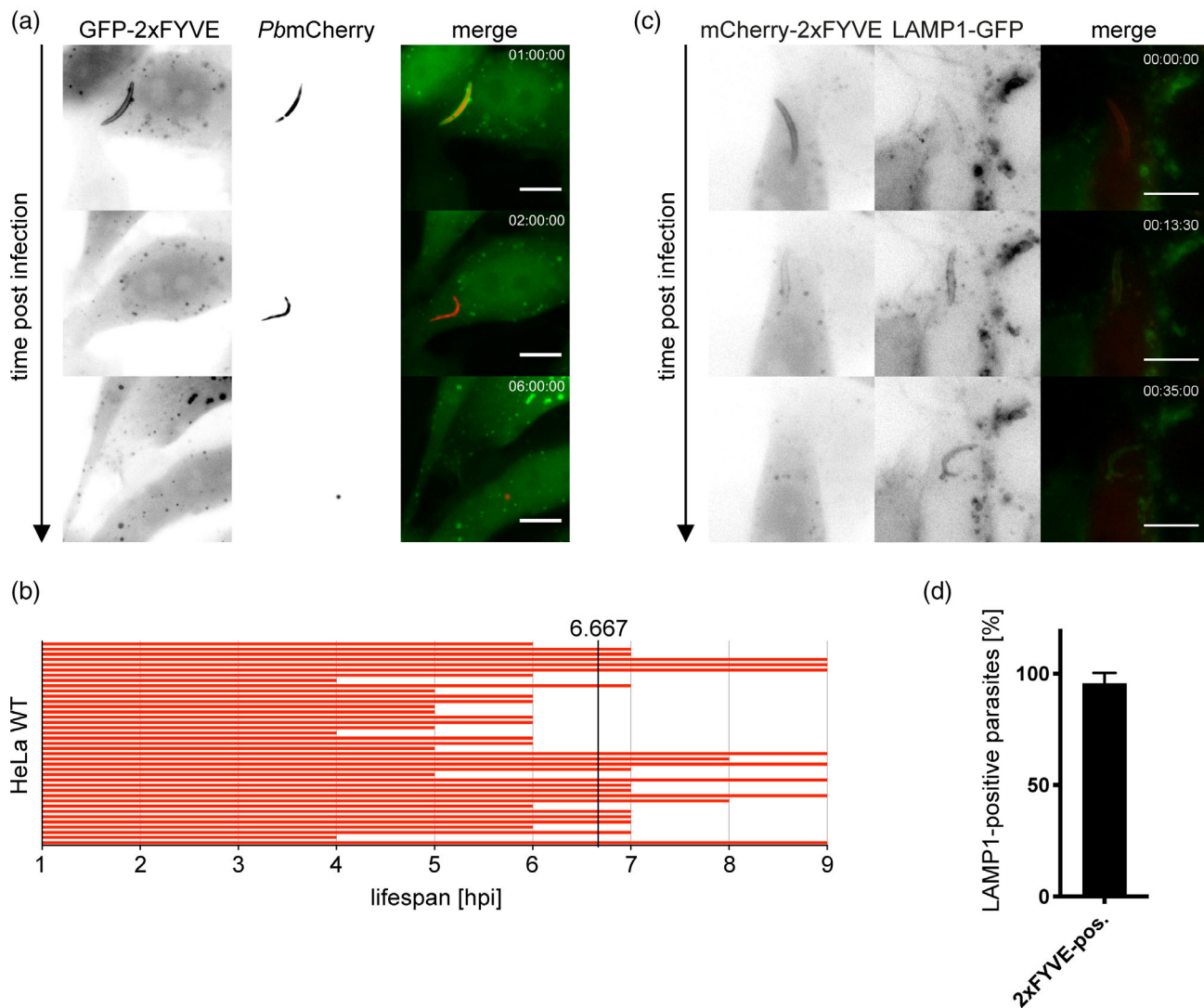
FIGURE 4 2xFYVE-positive parasites are efficiently eliminated. (a) GFP-2xFYVE-expressing HeLa cells were infected with *Pb*mCherry parasites. At 1 hpi, cells were washed to remove non-invaded sporozoites and time-lapse microscopy was performed at 30-min intervals. Still images of Movie S4 are depicted. Note the transient GFP-2xFYVE accumulation that is followed by disintegration of the parasite. Time stamps are in hh:mm:ss post infection. Scale bar: 10 μm. (b) Quantitative analysis of the life span of GFP-2xFYVE-positive parasites: time-lapse video microscopy was performed as described in (a) during the first 9 hr following sporozoite addition (see also Movie S4). Each line corresponds to one 2xFYVE-positive *Pb*mCherry parasite and ends when the parasite was eliminated, as determined by loss of mCherry fluorescence. The black vertical line shows the mean life span of 6.667 hr. $N = 39$ from two independent experiments. (c) HeLa cells co-expressing mCherry-2xFYVE and LAMP1-GFP were infected with *Pb*WT sporozoites. Upon addition of sporozoites, time-lapse imaging at 30-s intervals was performed. Still images of Movie S5 are shown. Note that the mCherry-2xFYVE-positive sporozoite becomes increasingly stained by LAMP1-GFP and arrests in development. $N = 12$. Time stamps are in hh:mm:ss post infection. Scale bar: 10 μm. (d) Quantification of (c). The percentage of 2xFYVE-positive parasites labelled with LAMP1-GFP was determined using movies as in (c). The graph depicts mean and *SD* of three independent experiments. $N = 13–27$ per experiment

parasites were also followed in HuH7 cells. Very similar as in HeLa cells, most of the parasites were eliminated in the first 7 hr after infection (Figure S3c,d and Movie S7). Next, we tested whether the observed acidification depends on the lipidation machinery of the host cell, which is a hallmark of LAP. We imaged 2xFYVE-positive *Pb*GFP parasites in HeLa cells deficient for the essential autophagy protein AUTOPHAGY-related 5 (ATG5) and observed a similar number of 2xFYVE-positive parasites in $ATG5^{-/-}$ host cells and in wild-type cells (Figure S5). Surprisingly, the majority of the parasites in

$ATG5^{-/-}$ cells lost their GFP fluorescence within a few hours, (Figure 5b,d and Movie S8) similar to parasites in wild-type, autophagy-competent host cells. This observation is a strong indication that the host cell response that targets 2xFYVE-positive parasites for acidification is independent of autophagy and related pathways such as LAP. As a control, we treated infected cells with chloroquine (CQ), which is a potent inhibitor of autophagosome–lysosome fusion (Mauthe et al., 2018) and is thus expected to prevent acidification of parasites. Indeed, upon CQ treatment of infected cells,
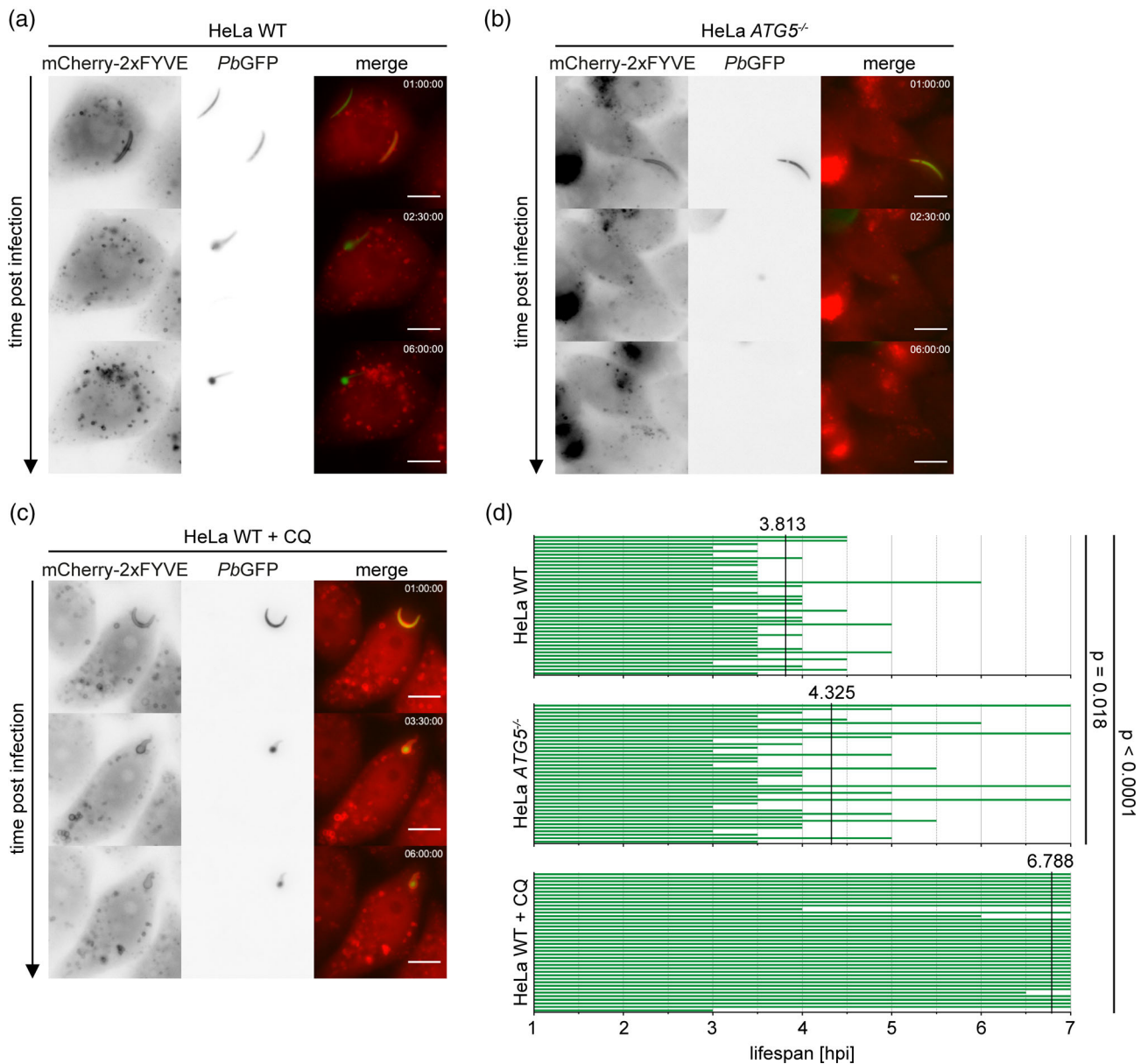
FIGURE 5 2xFYVE-positive parasites are eliminated independent of autophagy. (a) mCherry-2xFYVE-expressing HeLa cells were infected with *Pb*GFP parasites. At 1 hpi, cells were washed to remove excess sporozoites and time-lapse microscopy was performed at 30-min intervals. Still images of Movie S6 are depicted. A cell hosting two parasites is shown. Note that while the 2xFYVE-positive parasite loses fluorescence, the 2xFYVE-negative parasite begins transformation into a trophozoite. Time stamps are in hh:mm:ss post infection. Scale bar: 10 μm. (b) Experimental setup as in (a) but infection was performed using mCherry-2xFYVE-expressing autophagy-deficient (ATG5$^{-/-}$) HeLa cells. Still images of Movie S8 are depicted. Note the loss of parasite GFP fluorescence. Time stamps are in hh:mm:ss post infection. Scale bar: 10 μm. (c) Experimental setup as in (a) but WT HeLa cells were additionally treated with 100 μM chloroquine (CQ) from the time point of sporozoite addition. Still images of Movie S9 are depicted. Note that the GFP fluorescence is still visible 6 hpi in the 2xFYVE-positive parasite. Time stamps are in hh:mm:ss post infection. Scale bar: 10 μm. (d) Quantitative analysis of GFP fluorescence loss using movies such as those shown in (a)–(c) over the first 7 hr after sporozoite addition. Each line corresponds to one 2xFYVE-positive *Pb*GFP parasite and ends when GFP fluorescence was lost. Note that the fluorescence loss of 2xFYVE-positive *Pb*GFP parasites was faster (mean of 3.813 hr) compared to that for 2xFYVE-positive *Pb*mCherry parasites in Figure 3 (mean of 6.667 hr). This is because GFP, in contrast to mCherry, is sensitive to acidification. The black vertical lines show the mean timing of fluorescence loss for the observed parasites. *p*-Values were calculated using a Student's *t*-test. N = 40 per condition from two independent experiments

2xFYVE-positive parasites retained their GFP signal. These parasites even started to round up, which is a sign of development of the parasite into the trophozoite stage. However, these forms did not increase in size, suggesting that these parasites arrest in development (Figure 5c,d and Movie S9). In summary, these data obtained in ATG5-deficient and in CQ-treated host cells indicate that parasites

positive for PI3P are eliminated in an autophagy-independent but lysosome-dependent mechanism.

3 | DISCUSSION

Host cell autophagy and related processes are potent intracellular immune responses against pathogens (Paulus & Xavier, 2015). During development of *P. berghei* liver stages, the PVM is recognised by the hepatocyte and labelled with the autophagy marker LC3 (Grutzke et al., 2014; Prado et al., 2015; Thieleke-Matos et al., 2016). The majority of *P. berghei* liver stages show a strong, long-lasting LC3-labelling of their PVM (Grutzke et al., 2014; Prado et al., 2015; Thieleke-Matos et al., 2016; Wacker et al., 2017). LC3-labelling of the PVM and PAAR elimination of late liver stage schizonts, has been observed using live cell imaging (Prado et al., 2015). However, many *P. berghei* parasites successfully evade elimination by PAAR responses and successfully complete liver stage development (Prado et al., 2015). Parasites that develop successfully exhibit constant shedding of their PV membrane into the tubovesicular network (TVN), leading to a strong reduction in LC3-labelling towards the late schizont stage (Agop-Nersesian et al., 2017). The PAAR response against *P. berghei* involves LC3-association with the PVM and follows a non-canonical pathway with many similarities to LAP (Figure 6; Wacker et al., 2017). In contrast to canonical autophagy, the PAAR response is independent of the ULK complex and leads to direct incorporation of LC3 into the PVM (Martinez et al., 2011; Prado et al., 2015; Sanjuan et al., 2007; Wacker et al., 2017). LAP-like elimination of parasites infecting hepatocytes has been described for *Plasmodium vivax*, a human malaria parasite (Boonhok et al., 2016). *P. vivax*, in contrast to *P. berghei*, is not spontaneously recognised by the host cell autophagy machinery. Treatment of infected cells with IFNγ triggers labelling with LC3 in approximately 30% of the parasites and these are eliminated via a LAP-like pathway. We show here that for *P. berghei*, the majority of liver stage parasites are not recognised by the host cell via the classic LAP pathway. They rather provoke a PAAR response that is characterised by a long-lasting LC3-labelling of the PVM that is not preceded by PI3P-labelling. In addition to our observations, it was recently shown that LC3-association with the *P. berghei* PVM is independent of formation of reactive oxygen species (ROS), another hallmark of LAP (Real et al., 2018). Thus, despite sharing a similar molecular pathway, PAAR responses at the *P. berghei* PVM clearly differ from LAP. The observation of LAP-dependent and LAP-independent recognition of liver stages of *P. vivax* and *P. berghei* respectively, suggests that the nature of autophagy-related recognition of parasites can differ between different *Plasmodium* species which may reflect differences in development of liver stages. *P. vivax* can form dormant stages in the liver (Cogswell, 1992) and might have developed a mechanism to avoid immediate detection by the hepatocyte (Agop-Nersesian et al., 2018). An immediate response of the host cell as is observed for *P. berghei*, could be deleterious for the dormant *P. vivax* stage. To avoid elimination, the parasite must be able to constantly shed PV membrane in order to remove autophagy marker

proteins. Dormant forms with a strongly reduced metabolic activity may not be able to perform shedding as this process requires plenty of phospholipids and thus a very active metabolism.

PVM generation during productive invasion, which involves formation of a moving junction, includes removal of host plasma membrane proteins from the PVM and further remodelling by the parasite (Amino et al., 2008; Nyboer, Heiss, Mueller, & Ingmundson, 2018; Risco-Castillo et al., 2015; Spielmann et al., 2012). In addition to productively invading liver cells and forming a replicative PV, *Plasmodium* sporozoites can invade cells transiently during hepatocyte traversal (Mota et al., 2001; Risco-Castillo et al., 2015). In these hepatocytes, a TV membrane is established without the formation of a moving junction. Interestingly, it was previously shown that a proportion of sporozoites get trapped in their TV which are subsequently acidified and eliminated by their host cells (Risco-Castillo et al., 2015). However, how parasites are eliminated within TVs remained unclear. Here we provide evidence of a PI3P-associated sporozoite elimination (PASE) of such parasites by lysosomal acidification. As acidification of these parasites also occurs in autophagy-deficient (ATG5$^{-/-}$) cells, we conclude that this process is not or only partially autophagy-dependent. This also suggests that the PI3P-associated host cell response against transmigrating *Plasmodium* sporozoites also does not follow the classical LAP pathway or any other known autophagy pathway.

Since all sporozoites transmigrate through cells, a remaining question is why only a small percentage of this transmigrating parasites become PI3P-positive in their TV. An obvious explanation is that most sporozoites quickly exit the transmigrated cell and are therefore not recognised. Indeed, using SPECT2-deficient parasites that are not able to egress from their TV, we observed a much higher percentage of PI3P-positive parasites (around 50%). This supports the idea that the PI3P-dependent host response described in this study targets mainly sporozoites that are trapped in their nonreplicative TVs. While most of the parasites that become PI3P-positive are still RON4-positive, indicating the lack of discharge of their rhoptries, some parasites were found RON4-negative. These parasites may have attempted productive invasion of the host cell but since their PVM remains negative for the exported protein UIS4, they likely failed to remodel their PVM. A compromised PVM could render them vulnerable to host cell elimination mechanisms. It was already shown earlier that inhibition of parasite protein export during the liver stage is detrimental for correct formation of a PVM, leading to parasite death (Hanson et al., 2013). A non-functional PVM may allow the host cell to accumulate protons in the PV by fusion with lysosomes and thus acidify the parasite, whereas a fully competent PVM is able to prevent this for example by the formation of proton-permeable pores.

It has previously been shown that independent of autophagy, lysosomes associate to and fuse with functional PVMs (Niklaus et al., 2019; Petersen et al., 2017; Wacker et al., 2017). Fusion of the PVM with lysosomes even appears to be essential for parasite growth, providing the parasite with cholesterol (Petersen et al., 2017) and most likely with other metabolites (Niklaus et al., 2019). Interestingly, reduced recruitment of lysosomal markers to UIS4-deficient parasites suggests a role for UIS4 in lysosomal recruitment to or fusion with the PVM (Petersen et al., 2017). However, parasites in TVs neither export UIS4 into the surrounding
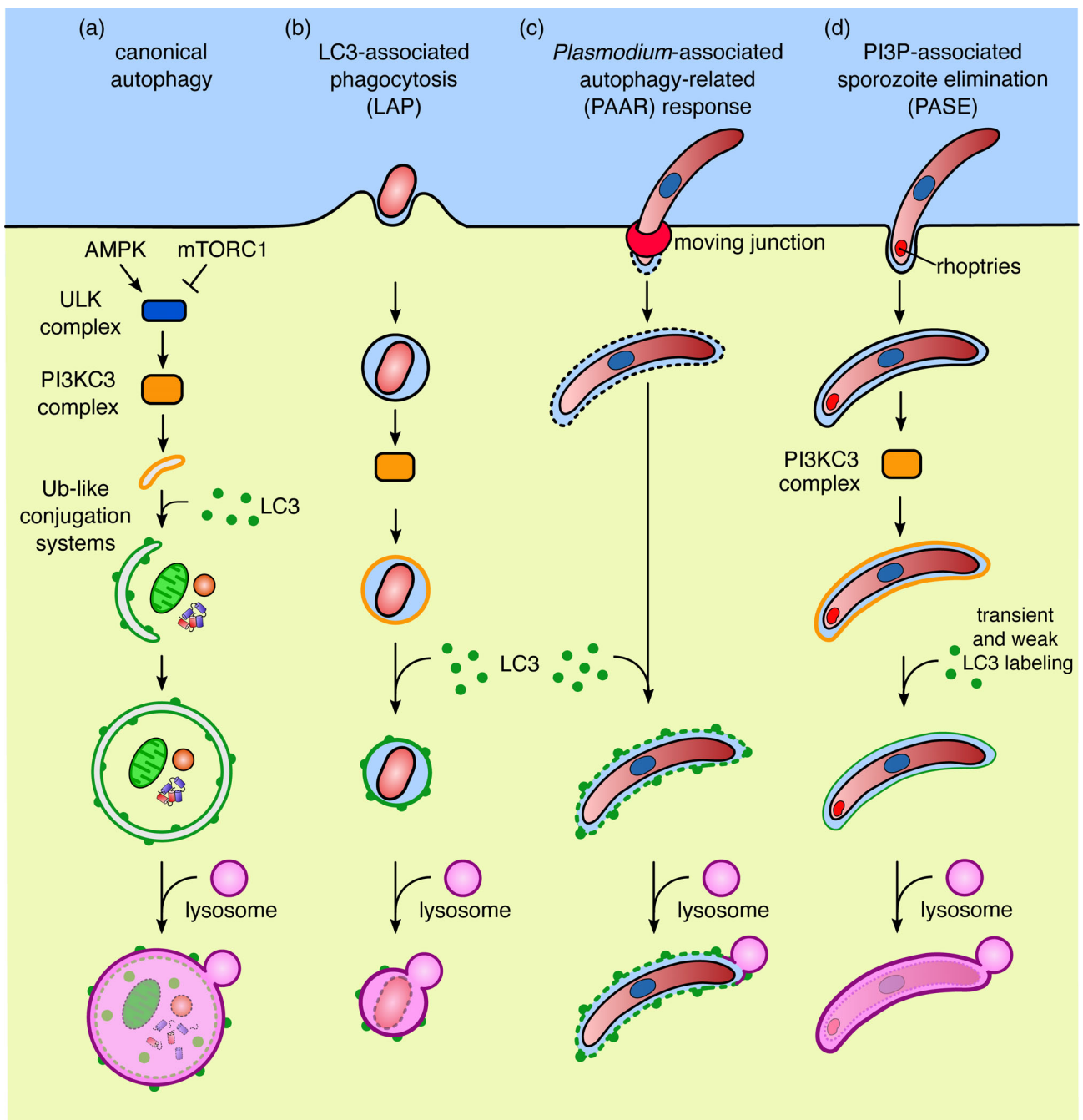
FIGURE 6 Schematic representation of the PAAR response and PASE in comparison to canonical autophagy and related pathways. (a) During starvation or stress conditions, autophagy is upregulated through a signalling pathway involving AMPK and mTORC1. Autophagosomes, double-membrane vesicles, engulf cytosolic substrates. Activation of the ULK1 complex activates PI phosphorylation to PI3P in the candidate membrane by a class III PI3K complex (PI3KC3). This recruits downstream effectors and eventually two ubiquitin-like conjugation systems that process and lipidate LC3 to a PE in the autophagosome membrane. This leads to elongation and closure of the autophagosome membrane. Subsequently, fusion with lysosomes leads to digestion of autophagosome contents. (b) LC3-associated phagocytosis (LAP) is an autophagy-related mechanism that leads to direct labelling of a single-membrane phagosome with autophagy proteins. PI3P and the production of ROS lead to recruitment of the ubiquitin-like conjugation systems and thus to LC3 integration into the phagosome membrane, to lysosome fusion and degradation of the phagosome contents. In contrast to canonical autophagy, LAP is independent of the ULK1 complex. (c) When *Plasmodium* parasites infect cells, they invaginate the host cell membrane, thus forming a parasitophorous vacuole (PV). This relies on discharge of proteins from apical organelles called rhoptries (red). Rhoptry proteins form a moving junction that sieves host cell membrane proteins during vacuole formation. The PV membrane (PVM) is heavily remodelled by the parasite and contains pores. During the PAAR response, the ubiquitin-like conjugation systems are recruited to the *Plasmodium* PVM and insert LC3. In contrast to other autophagy-related pathways, the PAAR response is independent of the ULK complex and the PI3KC3 complex. The PAAR response does not necessarily lead to elimination of the parasite, although lysosome markers are present at the PVM. (d) If parasites enter host cells without discharging their rhoptries and fail to exit or remodel their vacuole, PI3P is formed at the vacuole membrane. This leads to acquisition of lysosome markers and to acidification of the parasite. Although LC3 can be observed transiently at the vacuole membrane, its presence is not essential for efficient elimination of these parasites (adapted from (Agop-Nersesian et al., 2018))

membrane, nor attract long-lasting labelling of the vacuolar membrane with LC3. The TV membrane, however, remains still fusogenic for lysosomes and parasites are efficiently acidified. This suggests a mechanism for lysosome fusion that is independent of UIS4 and autophagy.

It has been shown that several bacterial pathogens modulate host phosphoinositide metabolism in order to establish their replicative niche. Some bacteria, for example, *Salmonella spp*, actively recruit PI3P to their vacuolar membrane, where it is thought to contribute to the enlargement of the vacuole by stimulating homotypic fusion with other PI3P-positive vesicles (Hernandez, Hueffer, Wenk, & Galan, 2004). In contrast, other bacteria avoid PI3P-labelling of their compartment. For example, *Mycobacterium tuberculosis* exports PI-metabolising enzymes that rapidly turn over PI3P in the vacuolar membrane. This keeps PI3P levels in the membrane constantly low thereby arresting the endocytic pathway, which is responsible for pathogen elimination (reviewed in [Weber, Ragaz, & Hilbi, 2009]). A similar mechanism could be used by *P. berghei*. It might be that PI3P at the PVM is further converted to PI(3,5)P_2 by host cell PIKFYVE, as PIKFYVE was shown to be present and active at the PVM of *P. berghei* parasites (Thieleke-Matos et al., 2014).

In this study, we show that PI3P-labelling of transmigrating *P. berghei* sporozoites strongly correlates with parasite elimination. We propose that this newly observed PI3P-dependent host cell response is part of a default recognition mechanism triggered in host cells to recognise, label and eliminate intracellular pathogens. While *Plasmodium* parasites residing in a fully functional PVM can evade elimination by the host cell, parasites that fail to remodel their vacuole membrane are still susceptible to the default host cell surveillance system. We show that the PI3P response ultimately results in parasite elimination and is clearly distinct from the typical PAAR response. The discovery of these two different cellular responses against *Plasmodium* parasites shows that the host cell has different means to eliminate pathogens and a better understanding of the corresponding pathways might help to discover new ways to effectively eliminate the parasite at this early stage of infection.

4 | EXPERIMENTAL PROCEDURES

4.1 | Experimental animals at University of Bern

Mice used in the experiments were between 6 and 10 weeks of age and were bred in the central animal facility of the University of Bern. Animal experiments were performed in strict accordance to the guidelines of the Swiss Tierschutzgesetz (TSchG; Animal Rights Laws) and approved by the ethical committee of the University of Bern (licence number: BE116/16 and BE86/19).

4.2 | Experimental animals at Leiden University Medical Center

Female OF1 mice (6–7 weeks; Charles River, NL) were used. All animal experiments of this study were approved by the Animal Experiments Committee of the Leiden University Medical Center (DEC

12042). All animal experiments of this study were granted with a licence by Competent Authority after an advise on the ethical evaluation by the Animal Experiments Committee Leiden (DEC12042). All experiments were performed in accordance with the Experiments on Animals Act (Wod, 2014), the applicable legislation in the Netherlands in accordance with the European guidelines (EU directive no. 2010/63/EU) regarding the protection of animals used for scientific purposes. All experiments were executed in a licenced establishment for use of experimental animals (LUMC).

4.3 | Common parasite strains

All parasite strains used have a *P. berghei* ANKA background. *Pb*mCherry and *Pb*GFP parasites are phenotypically wild-type like *Pb*WT. *Pb*mCherry express cytosolic mCherry under the control of the *P. berghei* hsp70 regulatory sequences (Burda et al., 2015). *Pb*GFP parasites express cytosolic GFP under the promoter of the eukaryotic elongation factor 1-alpha (eef1α; Franke-Fayard et al., 2004).

The reference 'wild-type' *P. berghei* ANKA parasite line, cl15cy1 (ANKAwt; Otto et al., 2014), was used for generating the RON4-mCherry line.

*Pb*Spect2(−)F parasites were a kind gift of Robert Ménard and were described previously (Amino et al., 2008; Ishino et al., 2005).

4.4 | Generation, selection and genotyping of a transgenic parasite expressing mCherry fluorescently tagged RON4

To generate the transgenic RON4-mCherry, parasites expressing C-terminally tagged mCherry RON4 (PBANKA_932000), construct pL1577 was used (Fougere et al., 2016). The *smac* (PBANKA_0100600) was exchanged for the *ron4* targeting region amplified with primers 6686 and 6687 (5′-gg**actagt**GCATCCATATTAATGCAACAATGG and 5′-ccc**ggatcc**TAAATCATCAAAAATGGCTTTCTC) using restriction sites, *Spe*I/*Bam*HI (Figure S4). Transfection (exp. 1964; RMgm-628; www.pberghei.eu) of the linearised pL1837 plasmid (using *Nde*I), selection and cloning of transformed parasites was performed using standard genetic modification technologies (Janse, Ramesar, & Waters, 2006) using ANKAwt parasite line. Correct integration of the DNA construct into the genome was verified by Southern analysis of Pulsed Field Gel (PFG)-separated chromosomes (Janse et al., 2006). PFG-separated chromosomes of the mutant line 1964 were hybridised with 3′UTR *Pbdhfr/ts* probe recognising the 3′UTR of the bifunctional dihydrofolate reductase-thymidylate synthase (dhfr/ts) gene of *P. berghei*. This probe recognises the endogenous 3′UTR of the *dhfr/ts* located on chromosome 7 and the 3′UTR of the integrated PL1837 construct into the *ron4* target gene located on chromosome 9 (Figure S4).

For analysis of mCherry expression of the RON4::mCherry line, infected tail blood was collected and *in vitro* cultured overnight in complete 1640-RPMI culture medium (Pasini et al., 2013). mCherry expression in schizonts was analysed by fluorescence microscopy

using a Leica DMR fluorescence microscope with standard Hoechst and Texas Red filters. Parasite nuclei were labelled by staining with Hoechst-33258 (2 μmol/L; Sigma, NL).

4.5 | Culture, treatment and *in vitro* infection of cells

HeLa cells (European Cell Culture Collection) and HuH7 cells (Japanese Collection of Research Bioresources Cell Bank JCRB0403) were cultured in Minimum Essential Medium with Earle's salts (MEM EBS; BioConcept, 1-31F01-I), supplemented with 10% FCS (GE Healthcare), 100 U penicillin, 100 μg/ml streptomycin, and 2 mM L-glutamine (all from Bioconcept). HeLa cells constitutively expressing GFP-LC3B were described before (Agop-Nersesian et al., 2017). To generate HeLa cells constitutively expressing LAMP1-GFP, the LAMP1-GFP open reading frame was amplified using primers 5′-ATCGGACCGATGGCGCCCCGCAG-3′ and 5′-ATCGGTCCGTTACTTGTACAGCTCG-3′ from a LAMP1-GFP expression vector kindly provided by John Brumell, Hospital for Sick Children, Toronto, Canada, and subcloned via *Rsr*II restriction sites in pRRLSIN. cPPT.PGK-GFP.WPRE. Virus production and transduction of cells were done as described previously for GFP-LC3B-expressing cells (Agop-Nersesian et al., 2017). The lentiviral expression plasmid pRRLSIN.cPPT. PGK-GFP.WPRE (Addgene plasmid #12252), as well as the VSV-G envelope-expressing plasmid pMD2.G (Addgene plasmid #12259) and the second-generation packaging plasmid psPAX2 (Addgene plasmid #12260) were gifts from Didier Trono. HeLa cells deficient for ATG5 were described before (Wacker et al., 2017). In order to perform live cell imaging with green and red fluorescence, the exogenous expression of GFP-LC3B in $ATG5^{-/-}$ cells was reversed by CRISPR/Cas9 with a guideRNA against GFP, a gift from George Church (Addgene plasmid 41819, [Mali et al., 2013]) together with the Cas9-expressing plasmid pX330, a gift from Feng Zhang (Addgene plasmid 42230, [Cong et al., 2013]). Cells were screened for absence of GFP fluorescence and five clones of non-fluorescent $ATG5^{-/-}$ cells were mixed to avoid clonal effects. Cells were cultured at 37°C and 5% CO_2 and split using Accutase (Innovative Cell Technologies) diluted 1:2 in phosphate-buffered saline (PBS; 137 mM NaCl, 2.7 mM KCl, 10 mM Na_2HPO_4, 1.8 mM KH_2PO_4, pH 7.4). For inhibitor treatments, HeLa cells were incubated in media containing 2.5 μM Wortmannin (Sigma-Aldrich W1628) or 100 μM CQ (Sigma-Aldrich C6628) for the indicated times. For infection of cells, salivary glands of infected *Anopheles stephensi* mosquitoes were isolated and disrupted to release sporozoites. Sporozoites were incubated with cells in the respective medium containing 25 μg/ml Amphotericin B (Amresco E437) for 2 hr. Subsequently, cells were washed with PBS and incubated in the respective medium containing 2.5 μg/ml Amphotericin B.

4.6 | Transfection of cells

HeLa or HuH7 cells were harvested by Accutase treatment and 1×10^6 cells were pelleted by centrifugation at 1,000*g* for 2 min at room temperature. Cells were resuspended in Nucleofector V solution (Lonza, VVCA-1003) and transfected with 1 μg of plasmid DNA using program T-028 of the Nucleofector 2b transfection device according to the manufacturer's instructions. The plasmid encoding RFP-LC3B was a generous gift of Tamotsu Yoshimori (Addgene plasmid 21075, [Kimura, Noda, & Yoshimori, 2007]). The plasmid used for expression of GFP-2xFYVE was kindly provided by Volker Haucke, FMP, Berlin, Germany. To generate the mCherry-2xFYVE expression plasmid, the 2xFYVE ORF was amplified using primers 5′-GAAAGCTTCGATGGAAAGTGATGCC-3′ and 5′-GAGGATCCTCATGCCTTCTTGTTCAG-3′ and subsequent subcloned into pmCherry-C1 (Clontech) using *Hind*III and *Bam*HI restriction sites.

4.7 | Indirect immunofluorescence analysis

After the indicated time periods, cells grown on glass cover slips were fixed with 4% paraformaldehyde in PBS for 10 min. Subsequently, they were permeabilised in 0.05% Triton X-100 (Fluka Chemie, T8787) in PBS for 5 min. Unspecific binding sites were blocked by incubation in 10% FCS/PBS for 10 min at room temperature. Cells were then incubated with primary antibody 1:500 in 10% FCS/PBS. The primary antibody used was rabbit anti-UIS4 antiserum (provided by P. Sinnis, Baltimore, MD). After washing with PBS, cells were incubated with fluorescently labelled secondary antibodies 1:2,000 in 10% FCS/PBS for 45 min. Secondary antibodies were anti-rabbit Alexa488 (Invitrogen, A11008) and anti-rabbit Cy5 (Dianova). DNA was visualised by staining with 1 μg/mL DAPI in PBS (Sigma-Aldrich) for 5 min. For filipin-staining, fixed cells without additional permeabilisation were incubated with 50 μg/ml filipin III (Sigma-Aldrich) in PBS for 45 min. All steps were carried out at room temperature. Labelled cells were mounted on microscope slides with Dako Fluorescence Mounting Medium (Dako, S3023).

4.8 | Quantification of parasites

HeLa cells expressing GFP-LC3 or GFP-2xFYVE infected with *P. berghei* parasites were fixed at the indicated time points and stained with the indicated stains or antibodies. Quantification was performed visually. Parasites were considered GFP-2xFYVE or filipin-positive if there was a clear ring of signal around the entire parasite. Parasites were considered UIS4-positive if UIS4 localised to the circumference of the parasite. Parasites exhibiting intracellular UIS4 were considered negative. Parasites were considered LC3-positive if the LC3 signal covered more than 30% of the area surrounding the parasite and colocalised with UIS4. For the quantification of RON4 discharge, parasites with an apical RON4-mCherry signal were counted as positive; parasites with dispersed or absent mCherry signal were considered negative. GraphPad Prism version 7 was used to draw graphs and to perform statistical analysis of quantifications.

4.9 | Microscopy

Live cell imaging was performed using an inverted Leica DMI6000B wide field epifluorescence microscope with a Leica HCX PL APO CS 63x1.2 water objective, with minimal light intensity and short illumination time. During imaging, cells were kept in 5% CO_2 at 37°C. Pictures were taken with the indicated intervals. Confocal images were acquired with an inverted Leica TCS SP8 using a HC PL APO CS2 63×/1.4 NA immersion oil objective. Analysis of fixed cells was done using a Leica DM5500B epifluorescence microscope or a Leica TCS SP8 confocal microscope with a HC PL APO CS2 63×/1.4 NA immersion oil objective. Pearson's correlation coefficient was calculated using the Coloc2 tool of the FIJI software. Image processing was performed using FIJI.

CONFLICT OF INTEREST

The authors declare no conflict of interests.

AUTHOR CONTRIBUTIONS

Annina Bindschedler, Rahel Wacker, Nina Eickel, Jessica Egli, Jacqueline Schmuckli-Maurer, Blandine M. Franke-Fayard and Chris J. Janse conducted the experiments. Volker T. Heussler supervised and coordinated the project. Annina Bindschedler, Rahel Wacker, Nina Eickel, Jessica Egli, Jacqueline Schmuckli-Maurer and Volker T. Heussler analysed the data. Annina Bindschedler, Rahel Wacker, Nina Eickel, Jacqueline Schmuckli-Maurer and Volker T. Heussler conceived and designed experiments. Annina Bindschedler, Rahel Wacker and Volker T. Heussler wrote the paper.

DATA AVAILABILITY STATEMENT

The data that support the findings of this study are available on request from the corresponding author.

ORCID

Annina Bindschedler https://orcid.org/0000-0003-0336-0864
Rahel Wacker https://orcid.org/0000-0002-0129-371X
Volker T. Heussler https://orcid.org/0000-0001-8028-9825

REFERENCES

Agop-Nersesian, C., De Niz, M., Niklaus, L., Prado, M., Eickel, N., & Heussler, V. T. (2017). Shedding of host autophagic proteins from the parasitophorous vacuolar membrane of *Plasmodium berghei*. *Scientific Reports*, 7(1), 2191. https://doi.org/10.1038/s41598-017-02156-7

Agop-Nersesian, C., Niklaus, L., Wacker, R., & Theo Heussler, V. (2018). Host cell cytosolic immune response during Plasmodium liver stage development. *FEMS Microbiology Reviews*, 42(3), 324–334. https://doi.org/10.1093/femsre/fuy007

Amino, R., Giovannini, D., Thiberge, S., Gueirard, P., Boisson, B., Dubremez, J. F., ... Menard, R. (2008). Host cell traversal is important for progression of the malaria parasite through the dermis to the liver. *Cell Host & Microbe*, 3(2), 88–96. https://doi.org/10.1016/j.chom.2007.12.007

Axe, E. L., Walker, S. A., Manifava, M., Chandra, P., Roderick, H. L., Habermann, A., ... Ktistakis, N. T. (2008). Autophagosome formation from membrane compartments enriched in phosphatidylinositol 3-phosphate and dynamically connected to the endoplasmic reticulum. *The Journal of Cell Biology*, 182(4), 685–701. https://doi.org/10.1083/jcb.200803137

Bano, N., Romano, J. D., Jayabalasingham, B., & Coppens, I. (2007). Cellular interactions of plasmodium liver stage with its host mammalian cell. *International Journal for Parasitology*, 37(12), 1329–1341. https://doi.org/10.1016/j.ijpara.2007.04.005

Besteiro, S., Dubremez, J. F., & Lebrun, M. (2011). The moving junction of apicomplexan parasites: A key structure for invasion. *Cellular Microbiology*, 13(6), 797–805. https://doi.org/10.1111/j.1462-5822.2011.01597.x

Boonhok, R., Rachaphaew, N., Duangmanee, A., Chobson, P., Pattaradilokrat, S., Utaisincharoen, P., ... Ponpuak, M. (2016). LAP-like process as an immune mechanism downstream of IFN-gamma in control of the human malaria *Plasmodium vivax* liver stage. *Proceedings of the National Academy of Sciences of the United States of America*, 113(25), E3519–E3528. https://doi.org/10.1073/pnas.1525606113

Burda, P. C., Roelli, M. A., Schaffner, M., Khan, S. M., Janse, C. J., & Heussler, V. T. (2015). A plasmodium phospholipase is involved in disruption of the liver stage parasitophorous vacuole membrane. *PLoS Pathogens*, 11(3), e1004760. https://doi.org/10.1371/journal.ppat.1004760

Chudakov, D. M., Matz, M. V., Lukyanov, S., & Lukyanov, K. A. (2010). Fluorescent proteins and their applications in imaging living cells and tissues. *Physiological Reviews*, 90(3), 1103–1163. https://doi.org/10.1152/physrev.00038.2009

Cogswell, F. B. (1992). The hypnozoite and relapse in primate malaria. *Clinical Microbiology Reviews*, 5(1), 26–35. https://doi.org/10.1128/cmr.5.1.26

Cong, L., Ran, F. A., Cox, D., Lin, S., Barretto, R., Habib, N., ... Zhang, F. (2013). Multiplex genome engineering using CRISPR/Cas systems. *Science*, 339(6121), 819–823. https://doi.org/10.1126/science.1231143

Fougere, A., Jackson, A. P., Bechtsi, D. P., Braks, J. A., Annoura, T., Fonager, J., ... Franke-Fayard, B. (2016). Variant exported blood-stage proteins encoded by plasmodium multigene families are expressed in liver stages where they are exported into the parasitophorous vacuole. *PLoS Pathogens*, 12(11), e1005917. https://doi.org/10.1371/journal.ppat.1005917

Franke-Fayard, B., Trueman, H., Ramesar, J., Mendoza, J., Keur, M., Linden, R., ... Janse, C. J. (2004). A *Plasmodium berghei* reference line that constitutively expresses GFP at a high level throughout the complete life cycle. *Molecular and Biochemical Parasitology*, 137(1), 23–33. https://doi.org/10.1016/j.molbiopara.2004.04.007

Gillooly, D. J., Morrow, I. C., Lindsay, M., Gould, R., Bryant, N. J., Gaullier, J. M., ... Stenmark, H. (2000). Localization of phosphatidylinositol 3-phosphate in yeast and mammalian cells. *The EMBO Journal*, 19(17), 4577–4588. https://doi.org/10.1093/emboj/19.17.4577

Grutzke, J., Rindte, K., Goosmann, C., Silvie, O., Rauch, C., Heuer, D., ... Ingmundson, A. (2014). The spatiotemporal dynamics and membranous features of the plasmodium liver stage tubovesicular network. *Traffic*, 15(4), 362–382. https://doi.org/10.1111/tra.12151

Hanson, K. K., Ressurreicao, A. S., Buchholz, K., Prudencio, M., Herman-Ornelas, J. D., Rebelo, M., ... Mota, M. M. (2013). Torins are potent antimalarials that block replenishment of plasmodium liver stage parasitophorous vacuole membrane proteins. *Proceedings of the National Academy of Sciences of the United States of America*, 110(30), E2838–E2847. https://doi.org/10.1073/pnas.1306097110

Hernandez, L. D., Hueffer, K., Wenk, M. R., & Galan, J. E. (2004). Salmonella modulates vesicular traffic by altering phosphoinositide metabolism. *Science*, 304(5678), 1805–1807. https://doi.org/10.1126/science.1098188

Huang, J., Canadien, V., Lam, G. Y., Steinberg, B. E., Dinauer, M. C., Magalhaes, M. A., ... Brumell, J. H. (2009). Activation of antibacterial autophagy by NADPH oxidases. *Proceedings of the National Academy of Sciences of the United States of America*, 106(15), 6226–6231. https://doi.org/10.1073/pnas.0811045106

Ishino, T., Chinzei, Y., & Yuda, M. (2005). A plasmodium sporozoite protein with a membrane attack complex domain is required for breaching the liver sinusoidal cell layer prior to hepatocyte infection. *Cellular Microbiology*, 7(2), 199–208. https://doi.org/10.1111/j.1462-5822.2004.00447.x

Ishino, T., Yano, K., Chinzei, Y., & Yuda, M. (2004). Cell-passage activity is required for the malarial parasite to cross the liver sinusoidal cell layer. *PLoS Biology*, 2(1), E4. https://doi.org/10.1371/journal.pbio.0020004

Janse, C. J., Ramesar, J., & Waters, A. P. (2006). High-efficiency transfection and drug selection of genetically transformed blood stages of the rodent malaria parasite *Plasmodium berghei*. *Nature Protocols*, 1(1), 346–356. https://doi.org/10.1038/nprot.2006.53

Kaiser, K., Matuschewski, K., Camargo, N., Ross, J., & Kappe, S. H. (2004). Differential transcriptome profiling identifies Plasmodium genes encoding pre-erythrocytic stage-specific proteins. *Molecular Microbiology*, 51(5), 1221–1232. https://doi.org/10.1046/j.1365-2958.2003.03909.x

Kimura, S., Noda, T., & Yoshimori, T. (2007). Dissection of the autophagosome maturation process by a novel reporter protein, tandem fluorescent-tagged LC3. *Autophagy*, 3(5), 452–460. https://doi.org/10.4161/auto.4451

Mali, P., Yang, L., Esvelt, K. M., Aach, J., Guell, M., DiCarlo, J. E., ... Church, G. M. (2013). RNA-guided human genome engineering via Cas9. *Science*, 339(6121), 823–826. https://doi.org/10.1126/science.1232033

Martinez, J., Almendinger, J., Oberst, A., Ness, R., Dillon, C. P., Fitzgerald, P., ... Green, D. R. (2011). Microtubule-associated protein 1 light chain 3 alpha (LC3)-associated phagocytosis is required for the efficient clearance of dead cells. *Proceedings of the National Academy of Sciences of the United States of America*, 108(42), 17396–17401. https://doi.org/10.1073/pnas.1113421108

Mauthe, M., Orhon, I., Rocchi, C., Zhou, X., Luhr, M., Hijlkema, K. J., ... Reggiori, F. (2018). Chloroquine inhibits autophagic flux by decreasing autophagosome-lysosome fusion. *Autophagy*, 14(8), 1435–1455. https://doi.org/10.1080/15548627.2018.1474314

Mizushima, N. (2010). The role of the Atg1/ULK1 complex in autophagy regulation. *Current Opinion in Cell Biology*, 22(2), 132–139. https://doi.org/10.1016/j.ceb.2009.12.004

Mota, M. M., Pradel, G., Vanderberg, J. P., Hafalla, J. C., Frevert, U., Nussenzweig, R. S., ... Rodriguez, A. (2001). Migration of *Plasmodium sporozoites* through cells before infection. *Science*, 291(5501), 141–144. https://doi.org/10.1126/science.291.5501.141

Nakatogawa, H. (2013). Two ubiquitin-like conjugation systems that mediate membrane formation during autophagy. *Essays in Biochemistry*, 55, 39–50. https://doi.org/10.1042/bse0550039

Niklaus, L., Agop-Nersesian, C., Schmuckli-Maurer, J., Wacker, R., Grunig, V., & Heussler, V. T. (2019). Deciphering host lysosome-mediated elimination of *Plasmodium berghei* liver stage parasites. *Scientific Reports*, 9(1), 7967. https://doi.org/10.1038/s41598-019-44449-z

Nyboer, B., Heiss, K., Mueller, A. K., & Ingmundson, A. (2018). The Plasmodium liver-stage parasitophorous vacuole: A front-line of communication between parasite and host. *International Journal of Medical Microbiology*, 308(1), 107–117. https://doi.org/10.1016/j.ijmm.2017.09.008

Otto, T. D., Bohme, U., Jackson, A. P., Hunt, M., Franke-Fayard, B., Hoeijmakers, W. A., ... Janse, C. J. (2014). A comprehensive evaluation of rodent malaria parasite genomes and gene expression. *BMC Biology*, 12, 86. https://doi.org/10.1186/s12915-014-0086-0

Pasini, E. M., Braks, J. A., Fonager, J., Klop, O., Aime, E., Spaccapelo, R., ... Franke-Fayard, B. (2013). Proteomic and genetic analyses demonstrate that *Plasmodium berghei* blood stages export a large and diverse repertoire of proteins. *Molecular & Cellular Proteomics*, 12(2), 426–448. https://doi.org/10.1074/mcp.M112.021238

Patterson, G. H., Knobel, S. M., Sharif, W. D., Kain, S. R., & Piston, D. W. (1997). Use of the green fluorescent protein and its mutants in quantitative fluorescence microscopy. *Biophysical Journal*, 73(5), 2782–2790. https://doi.org/10.1016/s0006-3495(97)78307-3

Paulus, G. L., & Xavier, R. J. (2015). Autophagy and checkpoints for intracellular pathogen defense. *Current Opinion in Gastroenterology*, 31(1), 14–23. https://doi.org/10.1097/mog.0000000000000134

Petersen, W., Stenzel, W., Silvie, O., Blanz, J., Saftig, P., Matuschewski, K., & Ingmundson, A. (2017). Sequestration of cholesterol within the host late endocytic pathway restricts liver-stage Plasmodium development. *Molecular Biology of the Cell*, 28(6), 726–735. https://doi.org/10.1091/mbc.E16-07-0531

Prado, M., Eickel, N., De Niz, M., Heitmann, A., Agop-Nersesian, C., Wacker, R., ... Heussler, V. T. (2015). Long-term live imaging reveals cytosolic immune responses of host hepatocytes against Plasmodium infection and parasite escape mechanisms. *Autophagy*, 11(9), 1561–1579. https://doi.org/10.1080/15548627.2015.1067361

Real, E., Rodrigues, L., Cabal, G. G., Enguita, F. J., Mancio-Silva, L., Mello-Vieira, J., ... Mota, M. M. (2018). Plasmodium UIS3 sequesters host LC3 to avoid elimination by autophagy in hepatocytes. *Nature Microbiology*, 3(1), 17–25. https://doi.org/10.1038/s41564-017-0054-x

Risco-Castillo, V., Topcu, S., Marinach, C., Manzoni, G., Bigorgne, A. E., Briquet, S., ... Silvie, O. (2015). Malaria sporozoites traverse host cells within transient vacuoles. *Cell Host & Microbe*, 18(5), 593–603. https://doi.org/10.1016/j.chom.2015.10.006

Risco-Castillo, V., Topcu, S., Son, O., Briquet, S., Manzoni, G., & Silvie, O. (2014). CD81 is required for rhoptry discharge during host cell invasion by *Plasmodium yoelii* sporozoites. *Cellular Microbiology*, 16(10), 1533–1548. https://doi.org/10.1111/cmi.12309

Russell, R. C., Tian, Y., Yuan, H., Park, H. W., Chang, Y. Y., Kim, J., ... Guan, K. L. (2013). ULK1 induces autophagy by phosphorylating Beclin-1 and activating VPS34 lipid kinase. *Nature Cell Biology*, 15(7), 741–750. https://doi.org/10.1038/ncb2757

Sanjuan, M. A., Dillon, C. P., Tait, S. W., Moshiach, S., Dorsey, F., Connell, S., ... Green, D. R. (2007). Toll-like receptor signalling in macrophages links the autophagy pathway to phagocytosis. *Nature*, 450 (7173), 1253–1257. https://doi.org/10.1038/nature06421

Schmuckli-Maurer, J., Reber, V., Wacker, R., Bindschedler, A., Zakher, A., & Heussler, V. T. (2017). Inverted recruitment of autophagy proteins to the *Plasmodium berghei* parasitophorous vacuole membrane. *PLoS ONE*, 12(8), e0183797. https://doi.org/10.1371/journal.pone.0183797

Spielmann, T., Montagna, G. N., Hecht, L., & Matuschewski, K. (2012). Molecular make-up of the Plasmodium parasitophorous vacuolar membrane. *International Journal of Medical Microbiology*, 302(4–5), 179–186. https://doi.org/10.1016/j.ijmm.2012.07.011

Sturm, A., Amino, R., Sand, C., Regen, T., Retzlaff, S., Rennenberg, A., ... Heussler, V. T. (2006). Manipulation of host hepatocytes by the malaria parasite for delivery into liver sinusoids. *Science*, 313(5791), 1287–1290. https://doi.org/10.1126/science.1129720

Tavares, J., Formaglio, P., Thiberge, S., Mordelet, E., Van Rooijen, N., Medvinsky, A., … Amino, R. (2013). Role of host cell traversal by the malaria sporozoite during liver infection. *The Journal of Experimental Medicine*, 210(5), 905–915. https://doi.org/10.1084/jem.20121130

Thieleke-Matos, C., da Silva, M. L., Cabrita-Santos, L., Pires, C. F., Ramalho, J. S., Ikonomov, O., … Barral, D. C. (2014). Host PI(3,5)P2 activity is required for *Plasmodium berghei* growth during liver stage infection. *Traffic*, 15(10), 1066–1082. https://doi.org/10.1111/tra.12190

Thieleke-Matos, C., Lopes da Silva, M., Cabrita-Santos, L., Portal, M. D., Rodrigues, I. P., Zuzarte-Luis, V., … Seabra, M. C. (2016). Host cell autophagy contributes to Plasmodium liver development. *Cellular Microbiology*, 18(3), 437–450. https://doi.org/10.1111/cmi.12524

Volinia, S., Dhand, R., Vanhaesebroeck, B., MacDougall, L. K., Stein, R., Zvelebil, M. J., … Waterfield, M. D. (1995). A human phosphatidylinositol 3-kinase complex related to the yeast Vps34p-Vps15p protein sorting system. *The EMBO Journal*, 14(14), 3339–3348.

Wacker, R., Eickel, N., Schmuckli-Maurer, J., Annoura, T., Niklaus, L., Khan, S. M., … Heussler, V. T. (2017). LC3-association with the parasitophorous vacuole membrane of *Plasmodium berghei* liver stages follows a noncanonical autophagy pathway. *Cellular Microbiology*, 19(10), 1–13. https://doi.org/10.1111/cmi.12754

Walker, S., Chandra, P., Manifava, M., Axe, E., & Ktistakis, N. T. (2008). Making autophagosomes: Localized synthesis of phosphatidylinositol 3-phosphate holds the clue. *Autophagy*, 4(8), 1093–1096. https://doi.org/10.4161/auto.7141

Weber, S. S., Ragaz, C., & Hilbi, H. (2009). Pathogen trafficking pathways and host phosphoinositide metabolism. *Molecular Microbiology*, 71(6), 1341–1352. https://doi.org/10.1111/j.1365-2958.2009.06608.x

Zhao, C., Liu, T., Zhou, T., Fu, Y., Zheng, H., Ding, Y., … Xu, W. (2016). The rodent malaria liver stage survives in the rapamycin-induced autophagosome of infected Hepa1-6 cells. *Scientific Reports*, 6, 38170. https://doi.org/10.1038/srep38170

SUPPORTING INFORMATION

Additional supporting information may be found online in the Supporting Information section at the end of this article.